

Chemistry A European Journal

 **Chemistry
Europe**
European Chemical
Societies Publishing

Accepted Article

Title: Photoswitching in a Liquid Crystalline Pt(II) Coordination Complex

Authors: Dan Wang, Jie Chen, Yixuan Wang, Xingtian Hao, Haiyan Peng, Yonggui Liao, Xingping Zhou, Ivan I. Smalyukh, and Xiaolin Xie

This manuscript has been accepted after peer review and appears as an Accepted Article online prior to editing, proofing, and formal publication of the final Version of Record (VoR). The VoR will be published online in Early View as soon as possible and may be different to this Accepted Article as a result of editing. Readers should obtain the VoR from the journal website shown below when it is published to ensure accuracy of information. The authors are responsible for the content of this Accepted Article.

To be cited as: *Chem. Eur. J.* **2024**, e202304366

Link to VoR: <https://doi.org/10.1002/chem.202304366>

Photoswitching in a Liquid Crystalline Pt(II) Coordination Complex

Dan Wang,^a Jie Chen,^a Yixuan Wang,^a Xingtian Hao,^a Haiyan Peng,^{a,b,c*} Yonggui Liao,^{a,b,c} Xingping Zhou,^{a,b,c} Ivan I. Smalyukh,^d Xiaolin Xie^{a,b,c*}

^a Key Lab of Material Chemistry for Energy Conversion and Storage, Ministry of Education, School of Chemistry and Chemical Engineering, Huazhong University of Science and Technology (HUST), Wuhan 430074, China

^b State Key Laboratory of Materials Processing and Die & Mould Technology, HUST, Wuhan 430074, China

^c National Anti-counterfeit Engineering Research Center, HUST, Wuhan 430074, China

^d Department of Physics and Materials Science and Engineering Program, University of Colorado at Boulder, Boulder, Colorado 80309, United States

Corresponding authors: hypeng@hust.edu.cn (H. Y. Peng), xlxie@hust.edu.cn (X. L. Xie)

Abstract: Photoswitching of photoluminescence has sparked tremendous research interests for super-resolution imaging, high-security-level anti-counterfeiting, and other high-tech applications. However, the excitation of photoluminescence is usually ready to trigger the photoswitching process, making the photoluminescence readout unreliable. Herein, we report a new photoswitch by the marriage of spiropyran with platinum(II) coordination complex. Viable photoluminescence can be achieved upon excitation by 480 nm visible light while the photoswitching can be easily triggered by 365 nm UV light. The feasible photoswitching may be benefited from the formed liquid crystalline phase of the designed photoswitch as a crystalline spiropyran is normally unable to implement photoswitching. Compared to the counterparts, this LC photoswitch can show distinct and reliable apparent colors and emission colors before and after photoswitching, which may promise the utility in high-security-level anti-counterfeiting and other advanced information technologies.

Keywords: Photoswitching, photochromism, photoluminescence, liquid crystal, platinum(II) complex, spiropyran

Introduction

Photoswitches normally represent molecules that can reversibly change their structural geometries in response to light, which have been of immense utility in a myriad of information technologies ranging from super-resolution bioimaging to molecule-scale magnetics, electronics and optoelectronics.^[1] However, it is normally difficult to enable multi-mode photoswitching in a single component.^[2] To tackle this difficulty, spiropyran (SP) derived photoswitches have been extensively studied in recent years as dual-mode photoswitching can be easily realized.^[3] Their transformation from the unconjugated SP form to the conjugated merocyanine (MC) form would lead to distinct spectral changes in both the absorption and photoluminescence.^[4] More excitingly, apart from fluorescence-type photoluminescence, room-temperature phosphorescence can be also afforded through molecular engineering,^[5] which would provide added degrees of freedom to expand the switching capabilities. Nevertheless, the excitation of photoluminescence in those photoswitches is ready to trigger the photoisomerization simultaneously, and the consequent molecular transformation would make the photoluminescence readout unreliable.

To provide an effective solution to this issue, it would be rational to separate the excitation wavelength of photoluminescence and photoisomerization via molecular engineering. One viable example was demonstrated by Xu and co-workers in 2022.^[3b] In this work, they designed a new photoswitch termed BOSA-SP, in which the photoluminescence was excited at a longer wavelength (e.g., 488 nm) while the

photoisomerization was triggered at a shorter wavelength (e.g., 365 nm). Thanks to the design, stable and programmable triple fluorescence switching was demonstrated in a single-molecule system.

With inspiration from Xu's work, we envisaged an alternative approach via the marriage of SP with supramolecular platinum(II) coordination complexes. These complexes with d^8 electron configuration and square-planar geometry have generated enormous attention in recent years.^[6] This is not only because of their attractive photoluminescence properties given by spin-orbit coupling between the metal center and peripheral ligands,^[7] but also due to the ease of spectral modulation in both absorption and emission through the manipulation of intermolecular π - π and Pt \cdots Pt interactions.^[8] As such, the excitation of photoluminescence would be possibly isolated from photoisomerization with careful molecular design, providing a new way to ensure nondestructive photoluminescence readouts in SP derivatives. In addition, the square-planar geometry makes Pt(II) complexes promising to be adapted for liquid crystal (LC) designs,^[9] an important pursuit as LC materials are fluidic smart soft matter with physical property anisotropy.^[10] They often exhibit appealing capabilities of delivering facile reversible and programmable responses to light or thermal stimuli.^[11] Nevertheless, despite the extensive exploration of LC Pt(II) complexes by anchoring flexible long alkyl chains that often aid to weaken the strong intermolecular stacking,^[9] photoswitchable LC Pt(II) complexes have been barely reported.

With the envision in mind, we herein reported an new example of photoswitchable LC Pt(II) complexes, namely Pt-SP (Figure 1), which was synthesized via coordination

reaction of the Pt(II) center with one primary *N,N,N*-tridentate ligand and another ancillary SP-functionalized pyridine ligand. This achievement can be ascribed to the beneficial chemical design: (1) The design provided an alternative route to imparting LC functions to metal coordination complexes other than alkylation with long alkyl chains.^[9] (2) Liquid crystallization made the intermolecular stacking less tight and thus facilitated the photoisomerization that was commonly difficult to take place in solid-state SP.^[3a] (3) Reliable nondestructive photoluminescence readouts were achieved due to the significant redshift of the “pump” wavelength from 365 to 480 nm while the “trigger” wavelength remained at 365 nm. This our work not only provides a viable paradigm to design multi-mode photoswitches but also showcases a novel approach to imparting LC functions to metal coordination complexes.

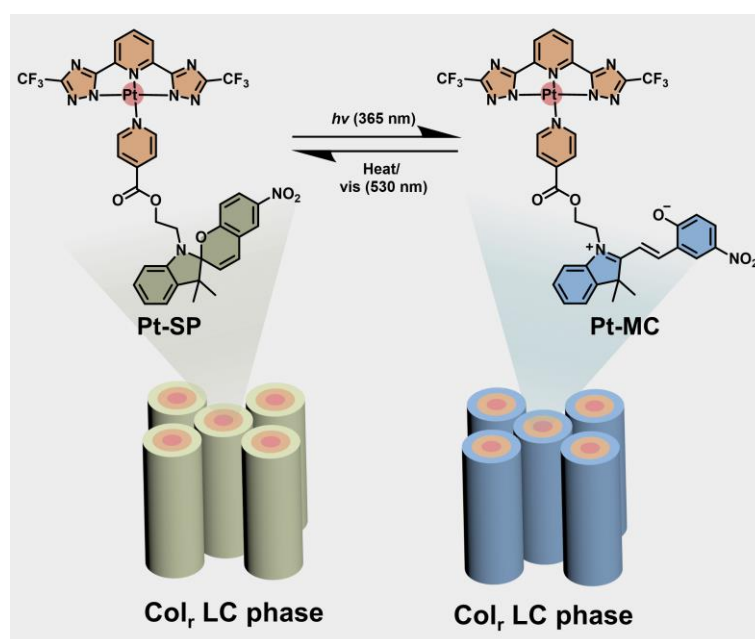


Figure 1. Schematic illustration of photoswitching in the designed LC Pt(II) coordination complex.

Results and Discussion

Synthesis of Pt-SP. Despite the unexpected LC characteristics afforded by the self-assembly of Pt-SP, the chemical design and synthesis began with the idea of spatiotemporal modulation of the photoluminescence of Pt(II) complexes by a photoswitchable unit. To this end, Pt-SP was synthesized via the efficient coordination reaction of $\text{PtCl}_2(\text{DMSO})_2$ with one primary *N,N,N*-tridentate ligand and another ancillary pyridyl ligand, based on the method pioneered by De Cola and co-workers.^[12] To reach the target product with the SP moiety, four-step separate reactions were implemented with varied yields from 55% to 90% (Scheme S1, Supporting Information). After purification, the target compound was identified by nuclear magnetic resonance (NMR) spectroscopy (e.g., ^1H NMR, ^{13}C NMR and ^{19}F NMR) and high-resolution mass spectrometry (HR-MS), following procedures as implemented in previous work.^[9d,12b]

Photophysical Properties. Once the target compound was ready, we evaluated its photophysical properties to lay the foundation for studying its photochemical performance. An intense absorption in the ultraviolet (UV) region was noted when Pt-SP was dissolved in dichloromethane (DCM, 0.01 mM, Figure S17), which could be attributed to the intraligand (^1IL) and metal-perturbed interligand charge transfer ($^1\text{ILCT}$), as displayed in other typical Pt(II) complexes.^[9d,12a] Interestingly, the absorption band was extended up to 450 nm in the visible region, primarily due to the admixture of spin-allowed intramolecular metal-to-ligand charge transfer ($^1\text{MLCT}$) and spin-forbidden $^3\text{MLCT}$ transitions.^[9d,12a] Upon photoexcitation at 420 nm, the solution

produced emissions at 464, 492, 525 and 568 nm, respectively, mainly assigned to the ligand-centered triplet excited state (^3LC) involving the tridentate chelate.^[9d,13] Besides, a significantly redshifted and increased emission was observed at 580 nm when the Pt-SP concentration was increased (Figure S17), which was attributed to metal-to-metal-to-ligand charge transfer ($^3\text{MMLCT}$) occurred in aggregated Pt(II) complexes.^[12b]

Photochemical Performance. Pt-SP underwent reversible photochemical reactions via photoisomerization. Under continuous UV light irradiation (365 nm, 0.5 mW/cm²), a new absorption band peaked at 592 nm gradually intensified for the Pt-SP solution in DCM (Figure 2a), giving origins to the generation of apparent color in light blue. The absorption change was attributed to transformation from the SP form to the MC form, and the latter possessed a more extended π -conjugation than the former.^[4b] The MC isomer seemed unstable in DCM and ready to undergo reverse transformation in dark, leading to quick absorption decay within 120 s (Figure 2b). At the same time, the apparent color was faded off. By contrast, such transformation was slowed down in bulk due to the tightened intermolecular stacking and restricted molecular motions.^[3a,14] As shown in Figure 2c, for the Pt-SP powder its transformation to the Pt-MC form was even incomplete after 420 s UV irradiation (365 nm, 0.5 mW/cm²). After transformation, the apparent color turned from dark yellow to dark brown associated with the significant increase of the absorption peak at 582 nm. This absorption was 10 nm blue-shifted and dramatically broadened compared to the absorption in DCM. Nevertheless, despite the reversibility of the transformation, the reverse transformation in powder was extremely slow under visible light illumination. Alternatively, the

reverse transformation could be complete in nearly 360 s upon heating to 100 °C (Figure 2d).

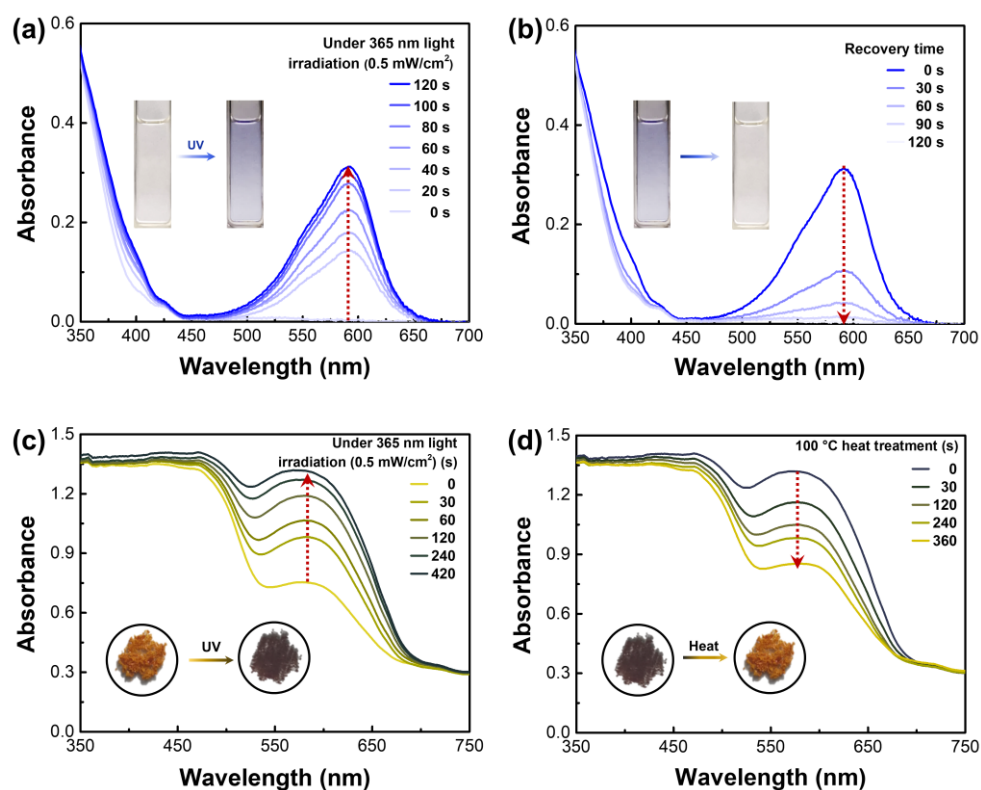


Figure 2. Absorption changes by transformation of Pt-SP. Absorption change of Pt-SP in DCM: (a) upon 365 nm light irradiation and (b) upon reversion in dark. Concentration: 0.01 mM. Absorption changes of Pt-SP powder: (c) upon 365 nm light irradiation and (d) upon heating. Insets: photographs taken under room light. UV-vis absorption for the Pt-SP powder was conducted by spectrophotometer with an integrating sphere.

The broad range of Pt-SP absorption in the visible region provided us the valuable opportunity to isolate the photoexcitation of photoluminescence from photoisomerization. For instance, a 480 nm light could be used to excite the photoluminescence at which the photoisomerization would not occur. As displayed in

Figure 3a, upon irradiation by 480 nm light the Pt-SP powder exhibited great emission band from 500 to 800 nm with two peaks at 585 and 645 nm, respectively. The former peak was ascribed to the pyridine-dominated $^3\text{MMLCT}$ of Pt(II) complexes in aggregation,^[9d,12b] while the latter was attributed to the SP-functionalized pyridine-dominated $^3\text{MMLCT}$. When lowering down the temperature from 298 to 78 K, the latter emission peak could be significantly intensified while the former was decayed (Figure S18), which was ascribed to tighter molecular stacking and Pt...Pt interactions. However, these emission peaks of Pt-SP were difficult to measure upon 365 nm light irradiation. Instead, a much weaker emission peaked at 680 nm was given due to the transformation from Pt-SP to Pt-MC via rapid photoisomerization. Figure 3b displays a further comparison. As clearly shown, the emission intensity at 585 nm was basically stable upon 480 nm light irradiation while sharply decreasing to zero upon 365 nm light irradiation, implying that nondestructive photoluminescence readouts could be achieved upon 480 nm light irradiation while photoswitching could be accomplished by 365 nm illumination. The photoswitching process could be timely monitored. As shown in Figure 3c, when irradiating the Pt-SP powder with UV light (365 nm, 0.5 mW/cm²), the original emission at 585 nm gradually diminished and the emission at 645 nm eventually redshifted to 685 nm, accompanied by intensity decrease. Interestingly, these emissions could recover upon heating the sample to 100 °C and keeping isothermal at this elevated temperature for 6 min, with good reversibility and high fatigue resistance (Figure 3d and S19).

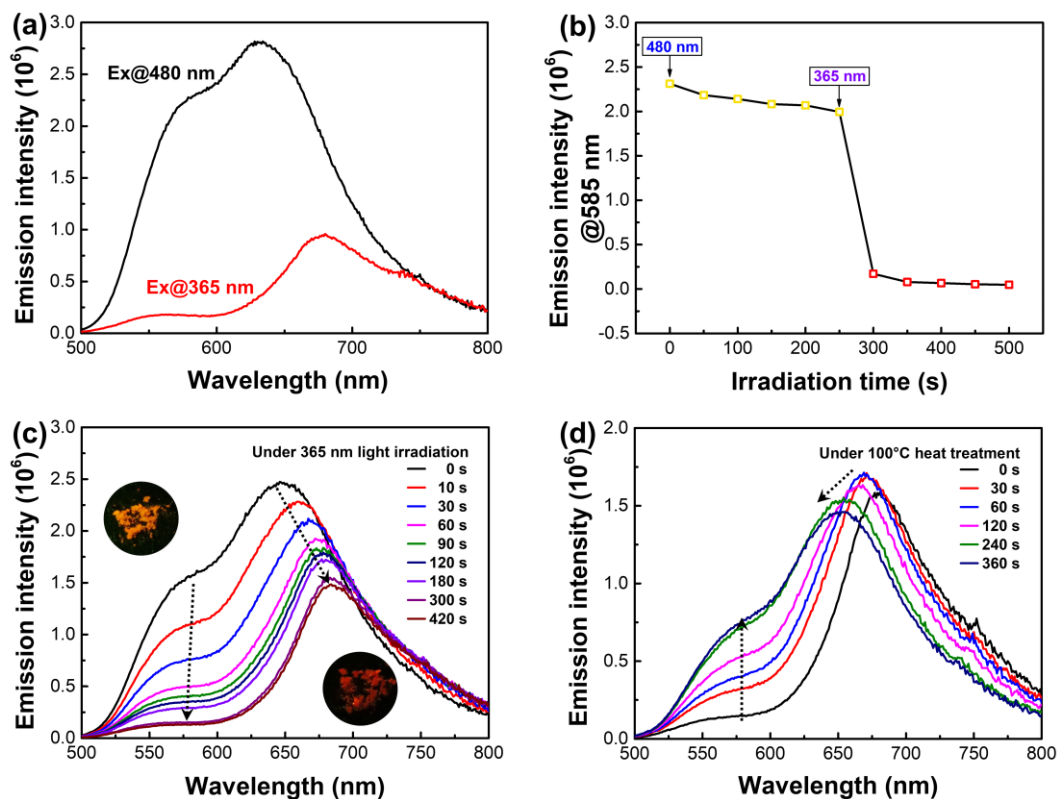


Figure 3. Nondestructive photoluminescence before and after photoisomerization.

(a) Emission spectra of the Pt-SP powders when excited by 480 and 365 nm, respectively. (b) Time-dependent emission of the Pt-SP powder under different excitation wavelengths. (c) Time-dependent emission spectra of the Pt-SP powder when irradiated by 365 nm light irradiation (0.5 mW/cm^2), and (d) emission recovery upon heating ($100 \text{ }^\circ\text{C}$). Excitation wavelength: 480 nm.

Mechanism of Switchable Photoluminescence. We suspected that the switchable intramolecular energy transfer was responsible for the switchable photoluminescence (Figure 4a), and then synthesized another Pt(II) complex without the SP moiety, namely, Pt-hexyl possessing a flexible hexyl chain (Figure 4b). As clearly shown, Pt-hexyl exhibited a single peak emission at 585 nm in powder, which was ascribed to the ³MMLCT of aggregated Pt(II) complexes.^[9d] This emission peak showed a significant

overlap with the absorption of MC rather than SP, implying possible intramolecular energy transfer from Pt center to the MC moiety. The condition for energy transfer was also satisfied by the small distance (Figure S20) between the Pt center and MC moiety.^[15] Lifetime measurements showed that during the transformation from the SP to MC form, the emission at 585 nm due to ³MMLCT was decreased by 16.3%, i.e., from 147 to 123 ns (Figure 4c), confirming efficient intramolecular energy transfer from the Pt center to the MC moiety.^[3b,14] Apart from the reversible change of emission spectra as aforementioned, the quantum yield (QY) also decreased due to the transformation. As illustrated in Figure 4d, the QY was decreased from 11% to 5% after transformation from the SP to MC form, indicating that an energy-transfer pathway can lead to a partial emission quenching.^[16] It is worth noting that the intramolecular electron transfer from the ancillary ligand to the Pt center could also lead to a decrease of QY. To show a clear picture, we implemented density functional theory (DFT) calculations. As shown in the bottom panel of Figure 4d, with respect to Pt-hexyl, both the lowest unoccupied molecular orbitals (LUMO) and highest occupied molecular orbitals (HOMO) were significantly contributed by orbitals of Pt centered moieties, indicating few chances for intramolecular electron transfer from the ancillary ligand to the Pt center and thus providing a high QY of 87%. In sharp contrast, the HOMO for both Pt-SP and Pt-MC was dominated by orbitals of the SP or MC moiety while the LUMO was governed by the Pt centered moieties, indicating a large probability of intermolecular electron transfer and resulting in relatively lower emission QY for both Pt-SP and Pt-MC.^[17]

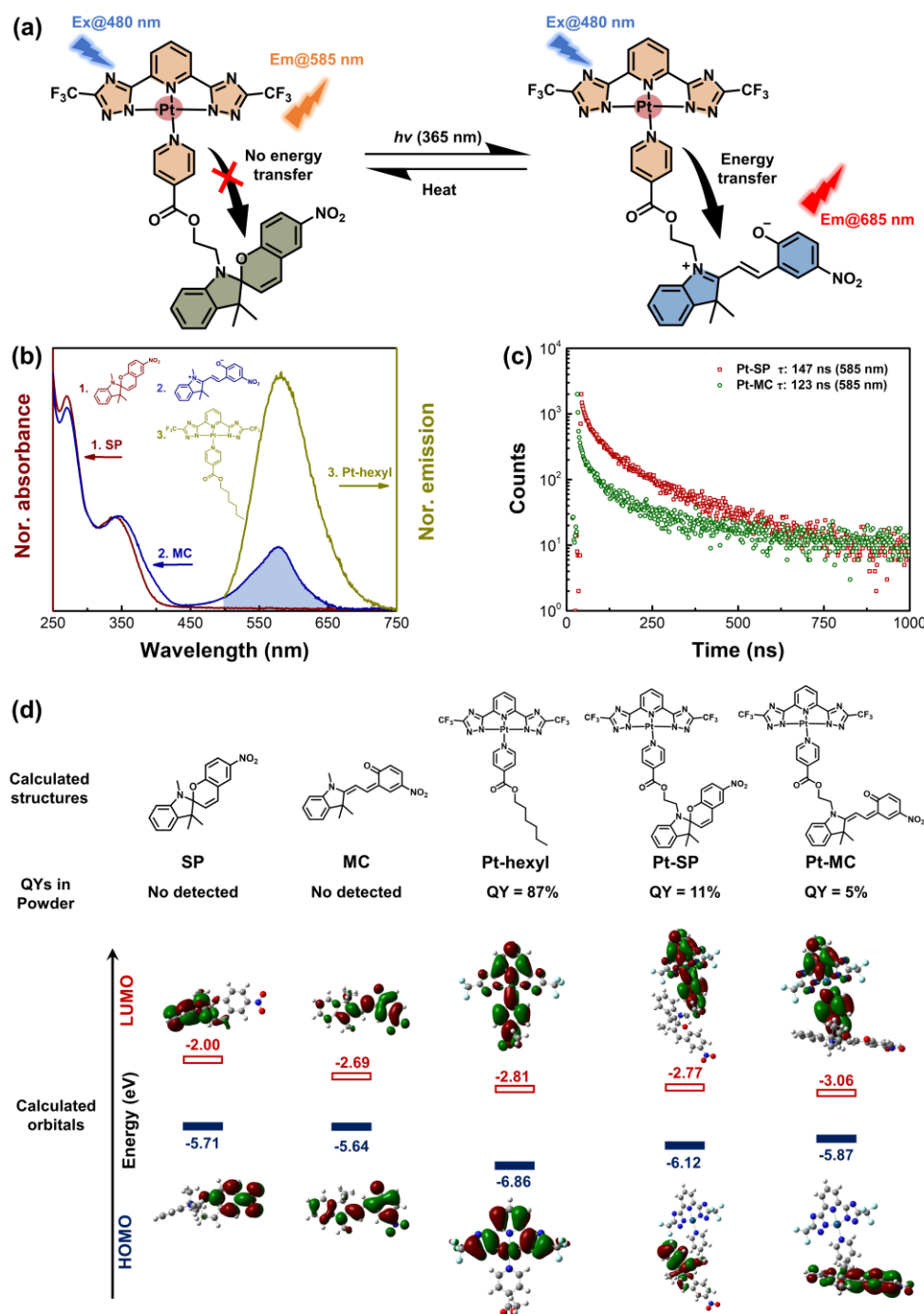


Figure 4. Photoswitching of Energy transfer. (a) Schematic illustration of energy transfer in Pt-SP and Pt-MC. (b) Spectra overlap between the SP and MC absorption and Pt-hexyl emission ($\lambda_{\text{ex}} = 480 \text{ nm}$). Nor. stands for normalized. The absorption was characterized in DCM solution (10^{-5} mol/L) while the emission was obtained in powder. (c) Emission decays of Pt-SP and Pt-MC powders (Excitation source: 450 nm laser). (d)

Calculated structures and orbitals, as well as QYs in powder for SP, MC, Pt-hexyl, Pt-SP and Pt-MC, respectively. Orbitals were calculated through the PBE1PBE1 functional in the DFT calculation. The alkyl chain in Pt-hexyl was simplified to methyl to save computation sources.

Photoswitching of LC textures. Unexpectedly, room-temperature LC phase rather than crystal phase was generated by supramolecular self-assembly of Pt-SP. Thermogravimetric analysis (TGA) proved a high thermal resistance of Pt-SP up to 300 °C under nitrogen atmosphere (Figure S21). The LC phase was characterized by combining polarized optical microscopy (POM), differential scanning calorimetry (DCS) and X-ray diffraction (XRD). POM images showed that the birefringence texture turned brighter upon heating and eventually disappeared at 160 °C (Figure S22), implying thermotropic phase transitions. Pt-SP was prone to flow upon heating, associated with the change of apparent color from dark yellow to bright green (Insets of Figure S22). The apparent color could be reversibly changed via alternate heating and cooling schemes. When cooled to room temperature from 160 °C, the complex changed from soft to rigid and harden into glassy state^[18] although no glass transition was observed in the DSC curves, and weak birefringence was observed in POM upon pressing (Figure S22). DCM vapor fuming promoted molecular orientation due to the perturbing effect of solvent molecules, resulting in a rapid generation of colored birefringence texture as observed from the POM. Since then, the color of textures could be reversibly switched upon alternate UV irradiation (365 nm, 0.5 mW/cm²) and 100 °C heating (Figure 5a). DCS curves only exhibited a very small or broad exothermic

transitions at 143 °C (enthalpy: 0.94 J/g) during the cooling process and a broad endothermic transition at 140 °C (enthalpy: 1.21 J/g) in the heating process (Figure 5b), which might be ascribed to the isotropic-mesophase transition. XRD results demonstrated the reversible switching of Pt-SP could be implemented within the same mesophase, and the Pt···Pt interaction distance^[8a,20] remained at 0.34 nm (Figure 5c). UV irradiation and thermal treatment under the temperature below the clearing point did not risk the molecular ordering according to unchanged sharp diffraction peaks in the small angle region. However, annealing from the isotropic phase substantially ruined the molecular ordering by weakening the intermolecular interactions, as evidenced by the broadened diffraction peaks and the shift of diffraction peak to small diffraction angles (Figure S23). These observations suggested that a metastable phase might emerge at low temperatures.^[19] These two separate diffraction peaks of Pt-SP/MC at the 2θ values of 5.50° and 9.16° and a broad peak at the wide angle range (25° ~ 29°) were distinct from those of SP crystal (Figure 5c and S23), implying the formation LC phase rather than soft crystal phase.^[19,21] According to the Bragg law,^[11e] the d -spacing was calculated to be 1.60 and 0.96 nm, respectively.

The LC phase was further identified by small-angle X-ray scattering (SAXS) analysis. As depicted in Figure 5d, three primary diffraction peaks were clear at the q values of 2.90, 3.92 and 6.54 nm⁻¹, respectively, giving rise to a q ratio of 1 : $\sqrt{2}$: $\sqrt{3}$ and thus confirming the formation of rectangular columnar (Col_r) phase. A Col_r phase is normally produced by distortion of hexagonal columnar (Col_h) phase. The three diffraction peaks with the d -spacing of 2.16, 1.60 and 0.96 nm could be indexed to the

(110), (200) and (130) facets of the CoI_r phase whose lattice parameters were calculated to be $a = 3.20$ nm and $b = 2.93$ nm, respectively, according to the equation 1,^[10,22]

$$1/d_{hkl}^2 = h^2/a^2 + k^2/b^2 \quad (1)$$

where, h , k and l denote the Miller indices.

The LC phase of the Pt-SP was unexpected as both the N,N,N -tridentate ligand and SP were crystalline (Figures S24 and S25). It also seemed that the chemical linking of the SP moiety is of essential significance for achieving the LC phase as the counterpart Pt-hexyl was also crystalline at room temperature (Figure S26). The partly twisted geometry of Pt-SP would account for the formation of the LC phase by loosing the molecular stacking (Figure S27). In other words, ordered stacking emerged due to the intermolecular $\text{Pt}\cdots\text{Pt}$ and π - π interactions while the twisted structure of SP prevent tightened stacking and crystallization. Since the fully extended conformation of Pt-SP exhibited smaller dimension (2.27 nm \times 1.53 nm, Figure S28) than the rectangular lattice parameters (3.20 nm \times 2.93 nm), around two molecules were included in one cell (see Section 1.5 in the Supporting Information). Therefore, we could imagine that Pt-SP/MC appears to be an atypical discoidal molecule, with the square-planar Pt(II) acting as a rigid central core providing intense $\text{Pt}\cdots\text{Pt}$ and π - π interactions while outside SP/MC moieties preventing crystallization (Figure 5e).^[9c] This type of molecular arrangement was the reason why facile photoswitching could be achieved with negligible change of the LC phase. As aforementioned, LC phases in Pt(II) complexes were basically obtained by anchoring flexible alkyl chains in previous work, the

marriage with SP moieties in this work could provide an alternative paradigm to impart LC functions to the complexes.

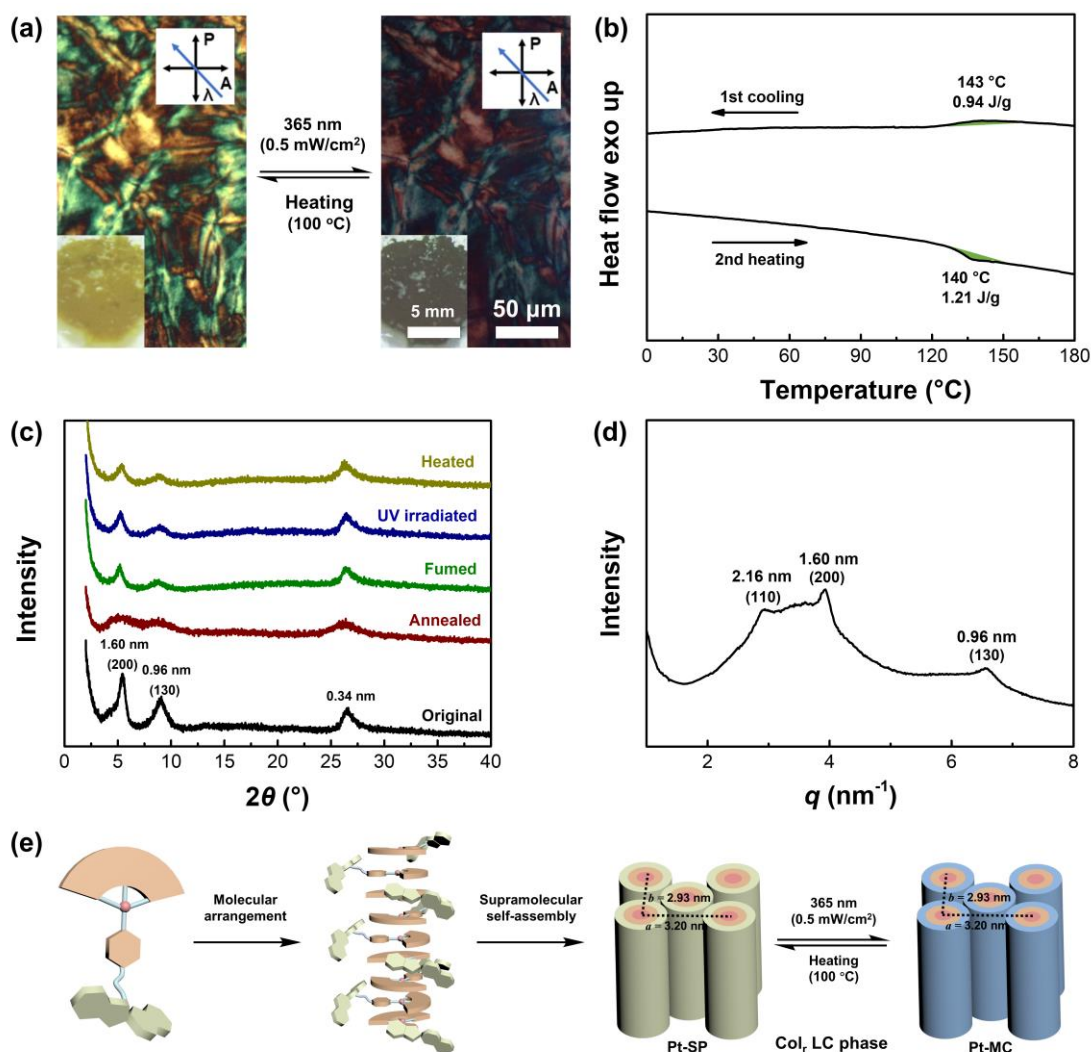


Figure 5. Thermotropic LC behaviors of the Pt-SP. (a) POM images of Pt-SP upon alternate UV irradiation and heating. A: analyzer, P: polarizer, λ : phase retardation plate. Insets of are images showing the change of apparent color and fluidity. (b) DSC curves of Pt-SP during the first cooling and second heating at ramp rate of 5 °C/min. (c) XRD patterns of Pt-SP at room temperature before and after different treatments. (d) SAXS pattern of as-prepared Pt-SP at room temperature. (e) Schematic illustration of the reasonable molecular self-assembly of Pt-SP/MC into the Col_r LC phase.

Photoswitchable Patterns. Thanks to the nondestructive readout of apparent color and photoluminescence in the LC phase, photoswitchable patterns could be achieved. As a proof-of-concept, patterns of “HG” were created by pouring the Pt-SP solution (50 mg/mL) into a mold and then removing the DCM solvent via volatilization in a hood (Figure 6a). As counterparts, Pt-hexyl and Py-SP (i.e., the ancillary ligand) were also shaped to “HG” patterns in a similar way. As illustrated in Figure 6b, when irradiating Pt-SP by 0.5 mW/cm² of 365 nm light, the apparent color changed from yellow to dark brown, the photoluminescence under 480 nm excitation changed from orange to red, and the color of LC texture changed from yellow to cyan-blue, due to the photoisomerization from the Pt-SP form to the Pt-MC form. All colors were reversible upon heating at 100 °C. In sharp contrast, no photoswitching could be achieved in Pt-hexyl, and no distinguishable photoluminescence could be produced at the same condition (Figure 6c). With respect to the counterpart Py-SP, insignificant photoluminescence can be achieved (Figure 6d). These results suggest the exclusive advantage of Pt-SP for high-security-level anti-counterfeiting and other high-tech applications in the information technology era.

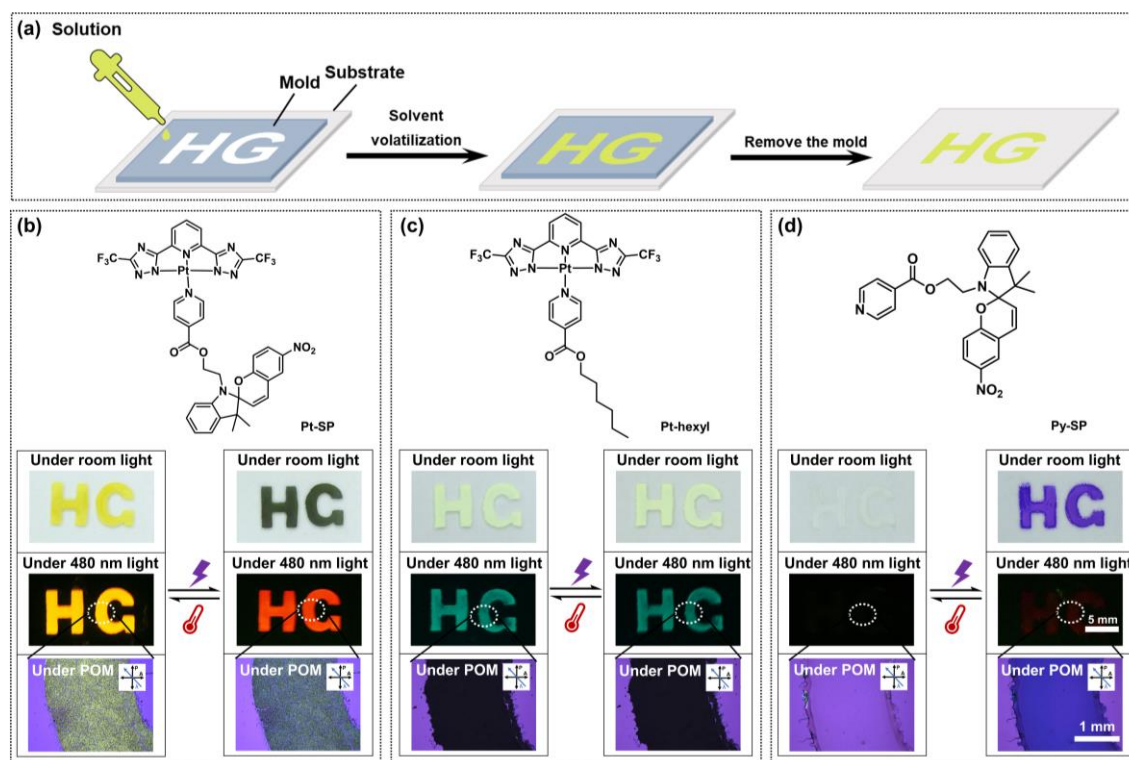


Figure 6. Photoswitching in the LC Pt(II) coordination complex. (a) Schematic illustration of the fabrication of message redout patterns. Photographs of pattern “HG” for: (b) Pt-SP, (c) Pt-hexyl and (d) Py-SP under room light, 480 nm light and POM, respectively. Symbols on arrows signified 365 nm irradiation (0.5 mW/cm^2) and the heating treatment ($100 \text{ }^\circ\text{C}$).

Conclusions

In summary, we have demonstrated an example of single-component photoswitch in Col_r LC phase, namely, the spiropyran decorated Pt(II) coordination complex Pt-SP. The spiropyran decoration provided an effective route to impart LC functions to metal coordination complexes other than previously common alkylation with long alkyl chains. Excitingly, the Pt-SP could display reversibly tunable apparent colors and photoluminescent colors via noninterference photoisomerization. The apparent color

changed from dark yellow to dark brown under 365 nm light irradiation. At the same time, the photoluminescent color under upon excitation of 480 nm changed from orange to red due to the “turn on” of intramolecular energy transfer. The displayed photoluminescent colors were reliable for both the open- and closed-isomers as the excitation wavelength was largely redshifted from 365 to 480 nm to eliminate side photoreactions. The photoswitching by Pt-SP can be easily recognized, which may promise immense technological utility in advanced anti-counterfeiting by eliminating illegal copy or imitation.

Supporting Information

The authors have cited additional references within the Supporting Information.^[23-28] Supporting Information is available that includes: synthesis and characterization; simulations; calculation of molecule number in a rectangular cell; absorption and emission spectra; photo-fatigue resistance; TGA curves; POM images; WAXS patterns; DSC curves; XRD patterns.

Acknowledgments

We thank the financial support from the National Key R&D Program of China (2023YFB3812404), the funds from the National Natural Science Foundation of China (52122316, 52073108 and 52233005), and the supports from the Innovation and Talent Recruitment Base of New Energy Chemistry and Device (B21003). We appreciate the technical support from the HUST Analytical & Testing Center, and Core Facilities of

Life Sciences. We would also like to thank Dr. Bijin Xiong from the School of Chemistry and Chemical Engineering at HUST for helping with the SAXS tests.

Conflict and Interest

The authors declare no conflict of interest.

References

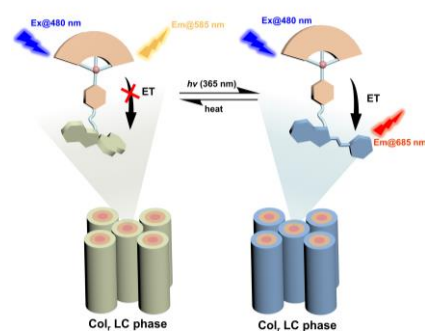
- [1] a) C. Jia, A. Migliore, N. Xin, S. Huang, J. Wang, Q. Yang, S. Wang, H. Chen, D. Wang, B. Feng, Z. Liu, G. Zhang, D.-H. Qu, H. Tian, M. A. Ratner, H. Q. Xu, A. Nitzan, X. Guo, *Science* **2016**, *352*, 1443-1445; b) J. Shou, A. Komazawa, Y. Wachi, M. Kawatani, H. Fujioka, S. J. Spratt, T. Mizuguchi, K. Oguchi, H. Akaboshi, F. Obata, R. Tachibana, S. Yasunaga, Y. Mita, Y. Misawa, R. Kojima, Y. Urano, M. Kamiya, Y. Ozeki, *Sci. Adv.* **2023**, *9*, eade9118; c) M. Irie, T. Fukaminato, T. Sasaki, N. Tamai, T. Kawai, *Nature* **2002**, *420*, 759-760; d) C. Li, A. Iscen, L. C. Palmer, G. C. Schatz, S. I. Stupp, *J. Am. Chem. Soc.* **2020**, *142*, 8447-8453; e) L. Qin, X. Liu, K. He, G. Yu, H. Yuan, M. Xu, F. Li, Y. Yu, *Nat. Commun.* **2021**, *12*, 699; f) L. Ma, G. Wang, B. Ding, X. Ma, *CCS Chem.* **2021**, *4*, 2080-2089; g) Z. Zheng, H. Hu, Z. Zhang, B. Liu, M. Li, D.-H. Qu, H. Tian, W.-H. Zhu, B. L. Feringa, *Nat. Photonics* **2022**, *16*, 226-234; h) B. Rösner, M. Milek, A. Witt, B. Gobaut, P. Torelli, R. H. Fink, M. M. Khusniyarov, *Angew. Chem. Int. Ed.* **2015**, *54*, 12976-12980; i) A. Fihey, A. Perrier, W. R. Browne, D. Jacquemin, *Chem. Soc. Rev.* **2015**, *44*, 3719-3759.
- [2] Y. Chen, Y. R. Lee, W. Wang, Y. Fang, S. Lu, J. Han, X. Chen, M. H. Kim, J. Yoon, *Angew. Chem. Int. Ed.* **2023**, *62*, e202301765.
- [3] a) Q. Qi, C. Li, X. Liu, S. Jiang, Z. Xu, R. Lee, M. Zhu, B. Xu, W. Tian, *J. Am. Chem. Soc.* **2017**, *139*, 16036-16039; b) R. Yang, X. Ren, L. Mei, G. Pan, X. Z. Li, Z. Wu, S. Zhang, W. Ma, W. Yu, H. H. Fang, C. Li, M. Q. Zhu, Z. Hu, T. Sun, B. Xu, W. Tian, *Angew. Chem. Int. Ed.* **2022**, *61*, e202117158; c) X. Wang, B. Xu, W. Tian, *Acc. Mater. Res.* **2023**, *4*, 311-322.

- [4] a) V. I. Minkin, *Chem. Rev.* **2004**, *104*, 2751-2776; b) R. Klajn, *Chem. Soc. Rev.* **2014**, *43*, 148-184; c) L. Kortekaas, W. R. Browne, *Chem. Soc. Rev.* **2019**, *48*, 3406-3424.
- [5] Y. Yang, A. Li, Y. Yang, J. Wang, Y. Chen, K. Yang, B. Z. Tang, Z. Li, *Angew. Chem. Int. Ed.* **2023**, e202308848.
- [6] a) Y. Han, Z. Gao, C. Wang, R. Zhong, F. Wang, *Coord. Chem. Rev.* **2020**, *414*, 213300; b) Z.-T. Shi, Y.-X. Hu, Z. Hu, Q. Zhang, S.-Y. Chen, M. Chen, J.-J. Yu, G.-Q. Yin, H. Sun, L. Xu, X. Li, B. L. Feringa, H.-B. Yang, H. Tian, D.-H. Qu, *J. Am. Chem. Soc.* **2021**, *143*, 442-452; c) F.-F. Xu, W. Zeng, M.-J. Sun, Z.-L. Gong, Z.-Q. Li, Y. S. Zhao, J. Yao, Y.-W. Zhong, *Angew. Chem. Int. Ed.* **2022**, *61*, e202116603.
- [7] a) H. Yersin, A. F. Rausch, R. Czerwiec, T. Hofbeck, T. Fischer, *Coord. Chem. Rev.* **2011**, *255*, 2622-2652; b) T. Theiss, S. Buss, I. Maisuls, R. López-Arteaga, D. Brünink, J. Kösters, A. Hepp, N. L. Doltsinis, E. A. Weiss, C. A. Strassert, *J. Am. Chem. Soc.* **2023**, *145*, 3937-3951.
- [8] a) V. C. Wong, C. Po, S. Y. Leung, A. K. Chan, S. Yang, B. Zhu, X. Cui, V. W. Yam, *J. Am. Chem. Soc.* **2018**, *140*, 657-666; b) M. H.-Y. Chan, V. W.-W. Yam, *J. Am. Chem. Soc.* **2022**, *144*, 22805-22825.
- [9] a) Y. X. Hu, X. T. Hao, L. Xu, X. L. Xie, B. J. Xiong, Z. B. Hu, H. T. Sun, G. Q. Yin, X. P. Li, H. Y. Peng, H. B. Yang, *J. Am. Chem. Soc.* **2020**, *142*, 6285-6294; b) V. N. Kozhevnikov, B. Donnio, D. W. Bruce, *Angew. Chem. Int. Ed.* **2008**, *47*, 6286-6289; c) M. Krikorian, S. Liu, T. M. Swager, *J. Am. Chem. Soc.* **2014**, *136*, 2952-2955; d) X. T. Hao, B. J. Xiong, M. L. Ni, B. Tang, Y. Ma, H. Y. Peng, X. P. Zhou, S. I. I., X. L. Xie, *ACS Appl. Mater. Interfaces* **2020**, *12*, 53058-53066; e) Z. Gao, Y. Han, F. Wang, *Nat. Commun.* **2018**, *9*, 3977.
- [10] C. Tschierske, *Angew. Chem. Int. Ed.* **2013**, *52*, 8828-8878.
- [11] a) T. Kosa, L. Sukhomlinova, L. Su, B. Taheri, T. J. White, T. J. Bunning, *Nature* **2012**, *485*, 347-349; b) J.-a. Lv, Y. Liu, J. Wei, E. Chen, L. Qin, Y. Yu, *Nature* **2016**, *537*, 179-184; c) H. Zhou, C. Xue, P. Weis, Y. Suzuki, S. Huang, K. Koynov, G. K. Auernhammer, R. Berger, H.-J. Butt, S. Wu, *Nat. Chem.* **2017**, *9*,

- 145-151; d) W. Hu, C. Sun, Y. Ren, S. Qin, Y. Shao, L. Zhang, Y. Wu, Q. Wang, H. Yang, D. Yang, *Angew. Chem. Int. Ed.* **2021**, *60*, 19406-19412; e) Y. X. Wang, Y. Liu, X. T. Hao, X. P. Zhou, H. Y. Peng, Z. H. Shen, I. I. Smalyukh, X. L. Xie, B. Yang, *Adv. Mater.* **2023**, *35*, 2303680; f) J. Li, S. Xie, J. Meng, Y. Liu, Q. Zhan, Y. Zhang, L. Shui, G. Zhou, L. Feringa Ben, J. Chen, *CCS Chem.* **2023**, 1-29; g) H. K. Bisoyi, Q. Li, *Chem. Rev.* **2016**, *116*, 15089-15166.
- [12] a) S. Carrara, A. Aliprandi, C. F. Hogan, L. De Cola, *J. Am. Chem. Soc.* **2017**, *139*, 14605-14610; b) A. Aliprandi, M. Mauro, L. De Cola, *Nat. Chem.* **2016**, *8*, 10-15.
- [13] M. Mauro, A. Aliprandi, C. Cebrián, D. Wang, C. Kübel, L. De Cola, *Chem. Commun.* **2014**, *50*, 7269-7272.
- [14] R. Yang, Y. Jiao, B. Wang, B. Xu, W. Tian, *J. Phys. Chem. Lett.* **2021**, *12*, 1290-1294.
- [15] C.-B. Huang, L. Xu, J.-L. Zhu, Y.-X. Wang, B. Sun, X. Li, H.-B. Yang, *J. Am. Chem. Soc.* **2017**, *139*, 9459-9462.
- [16] M. Tomasulo, E. Deniz, R. J. Alvarado, F. M. Raymo, *J. Phys. Chem. C* **2008**, *112*, 8038-8045.
- [17] a) S. Mo, Q. Meng, S. Wan, Z. Su, H. Yan, B. Z. Tang, M. Yin, *Adv. Funct. Mater.* **2017**, *27*, 1701210; b) Z. Wu, K. Pan, S. Mo, B. Wang, X. Zhao, M. Yin, *ACS Appl. Mater. Interfaces* **2018**, *10*, 30879-30886.
- [18] a) J. Kelber, M.-F. Achard, F. Durola, H. Bock, *Angew. Chem. Int. Ed.* **2012**, *51*, 5200-5203; b) A. Concellón, R.-Q. Lu, K. Yoshinaga, H.-F. Hsu, T. M. Swager, *J. Am. Chem. Soc.* **2021**, *143*, 9260-9266.
- [19] Y. Ren, W. H. Kan, M. A. Henderson, P. G. Bomben, C. P. Berlinguette, V. Thangadurai, T. Baumgartner, *J. Am. Chem. Soc.* **2011**, *133*, 17014-17026.
- [20] X. Zheng, H.-Y. Chan Michael, K.-W. Chan Alan, S. Cao, M. Ng, K. Sheong Fu, C. Li, C. Goonetilleke Eshani, Y. Lam William Wai, T.-C. Lau, X. Huang, W.-W. Yam Vivian, *Proc. Natl. Acad. Sci. U. S. A.* **2022**, *119*, e2116543119.

- [21] a) J. W. Goodby, R. J. Mandle, E. J. Davis, T. Zhong, S. J. Cowling, *Liq. Cryst.* **2015**, *42*, 593-622; b) M. Lehmann, S. Gloza, S. Roth, *Chem. Mater.* **2015**, *27*, 8181-8184.
- [22] S. Laschat, A. Baro, N. Steinke, F. Giesselmann, C. Hagele, G. Scalia, R. Judele, E. Kapatsina, S. Sauer, A. Schreivogel, M. Tosoni, *Angew. Chem. Int. Ed.* **2007**, *46*, 4832-4887.
- [23] M. El Garah, S. Sinn, A. Dianat, A. Santana-Bonilla, R. Gutierrez, L. De Cola, G. Cuniberti, A. Ciesielski, P. Samori, *Chem. Commun.* **2016**, *52*, 11163-11166.
- [24] S. Sinn, F. Biedermann, L. De Cola, *Chem. Eur. J.* **2017**, *23*, 1965-1971.
- [25] G. W. T. M. J. Frisch, H. B. Schlegel, G. E. Scuseria, M. A. Robb, J. R. Cheeseman, G. Scalmani, V. Barone, G. A. Petersson, H. Nakatsuji, X. Li, M. Caricato, A. Marenich, J. Bloino, B. G. Janesko, R. Gomperts, B. Mennucci, H. P. Hratchian, J. V. Ortiz, A. F. Izmaylov, J. L. Sonnenberg, D. Williams-Young, F. Ding, F. Lipparini, F. Egidi, J. Goings, B. Peng, A. Petrone, T. Henderson, D. Ranasinghe, V. G. Zakrzewski, J. Gao, N. Rega, G. Zheng, W. Liang, M. Hada, M. Ehara, K. Toyota, R. Fukuda, J. Hasegawa, M. Ishida, T. Nakajima, Y. Honda, O. Kitao, H. Nakai, T. Vreven, K. Throssell, J. A. Montgomery, Jr., J. E. Peralta, F. Ogliaro, M. Bearpark, J. J. Heyd, E. Brothers, K. N. Kudin, V. N. Staroverov, T. Keith, R. Kobayashi, J. Normand, K. Raghavachari, A. Rendell, J. C. Burant, S. S. Iyengar, J. Tomasi, M. Cossi, J. M. Millam, M. Klene, C. Adamo, R. Cammi, J. W. Ochterski, R. L. Martin, K. Morokuma, O. Farkas, J. B. Foresman, and D. J. Fox, Gaussian 09, Revision D.01, Gaussian, Inc., Wallingford CT, **2016**.
- [26] a) C. Adamo, V. Barone, *J. Chem. Phys.* **1999**, *110*, 6158-6170; b) M. M. Francl, W. J. Pietro, W. J. Hehre, J. S. Binkley, M. S. Gordon, D. J. DeFrees, J. A. Pople, *J. Chem. Phys.* **1982**, *77*, 3654-3665.
- [27] A. Bondi, *J. Phys. Chem.* **1964**, *68*, 441-451.
- [28] T. Lu, F. Chen, *J. Comput. Chem.* **2012**, *33*, 580-592.

-
- [29] a) H. Blanco, V. Iguarbe, J. Barbera, J. L. Serrano, A. Elduque, R. Gimenez, *Chem. Eur. J.* **2016**, *22*, 4924-4930; b) S. Moyano, J. Barberá, B. E. Diosdado, J. L. Serrano, A. Elduque, R. Giménez, *J. Mater. Chem. C* **2013**, *1*, 3119-3128.

ToC figure

An example of single-component multimode photoswitch was demonstrated by designing a novel Pt(II) coordination complex decorated with spiropyran, which can deliver distinct apparent colors, photoluminescent colors and liquid crystal textures in response to light.